

# Development of Mirror Segments for the Constellation-X Observatory

William Zhang, Kai-Wing Chan\*, David Content, Scott Owens, Robert Petre, Peter Serlemitsos, Timo Saha, and Yang Soong\*  
NASA's Goddard Space Flight Center, Greenbelt, MD 20771  
\*also Universities Space Research Association

## Abstract

As NASA's next major X-ray observatory, Constellation-X will have a photon collection area of  $30,000 \text{ cm}^2$  at 1 keV, which, after folding other instrumental responses, translates into an effective area of  $15,000 \text{ cm}^2$ . The observatory consists of four identical satellites each of which carries a spectroscopic X-ray telescope mirror assembly (SXT) that is 1.6 m in diameter and has a focal length of 10 m and a collection area of  $7,500 \text{ cm}^2$  at 1 keV and an angular resolution of  $15''$  HPD (half-power diameter) at the system level. Each mirror assembly consists of a large number of mirror segments precisely assembled together. Our development of the mirror segments is divided into two steps. The first one is to develop the basic approach and fabricate segments within the constraints of existing infra-structure to meet the angular resolution requirement, but not mirror segment size requirement. We have all but successfully completed this part of the development. We are now on the verge of going into the second step, that is to fabricate mirror segments of larger sizes to reduce the number of segments that have to be aligned and integrated. In this paper, we report on the requirements and the development status of the mirror segments. These assembly and other requirements of the SXT are reported elsewhere (Podgorski et al. and Hair et al.).

## 1 Introduction

Every X-ray telescope mirror assembly represents a compromise among four factors: (1) angular resolution, (2) effective area, (3) mass, and (4) production cost. The SXT mirror assemblies for the Constellation-X Observatory are no exception. Table 1 lists the requirements that SXT mirror assemblies must meet. They are derived from mission science requirements, mission systems level design considerations, as well as the state of the art of many relevant technologies.

**Table 1 Top level requirements of SXT mirror assemblies.**

Number of identical SXT Mirror Assemblies Required	4
Mirror Assembly Diameter	1,600 mm
Angular Resolution (End-to-End System)	$15''$ half-power diameter
Angular Resolution (Mirror Assembly Alone)	$10''$ half-power diameter

Effective Area at 1 keV per Assembly	$\geq 7,500 \text{ cm}^2$
Total Mass per Assembly	$< 719 \text{ kg}$

Figure 1 shows the top level design of the SXT assembly. It has 230 nested shells<sup>□</sup>. The primary and secondary shells each have a height in the optical axis direction of 200 mm. The entire assembly is segmented into 36 modules, 18 (6 inner and 12 outer) primary modules and 18 (6 inner and 12 outer) secondary modules. Tentatively, the division between the inner modules and the outer modules is set at shell 100 (counting inward from the largest shell). The inner modules have 130 segments each and the outer modules have 100 segments each. The total number of mirror segments required for each SXT mirror assembly is therefore:  $2 \times (12 \times 100 + 6 \times 130) = 3,960$ . In terms of linear dimensions, the smallest mirror segment measures about 150mm (60° in azimuth)  $\times$  200mm (optical axis) and the largest 418mm (30° in azimuth)  $\times$  200mm (optic axis).

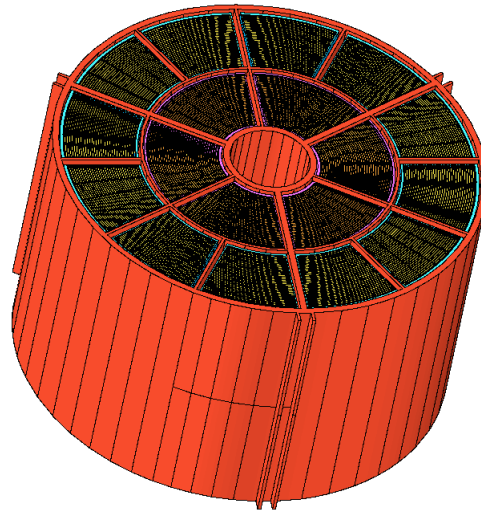


**Figure 1 The top level design of the SXT assembly. The entire assembly is segmented into 36 modules, 18 primary and 18 secondary ones. Only the 18 primary modules are visible in this view**

The challenge of constructing the SXT assemblies is two fold: fabrication of a large number (15,840) of precision mirror segments and accurately assembling them together. In this paper we report on the development of the mirror segments. Precision mounting of those mirror segments into the SXT assemblies are reported elsewhere (Podgorski et al. and Hair et al. these proceedings).

<sup>□</sup> For the sake of clarity in discussion, in this paper we assume a mirror segment axial length of 200mm. The axial length for flight design will be arrived at after taking into account several factors: mirror fabrication process, metrology, alignment complexity, etc. Currently we expect this length to be between 200 and 300mm. As of the writing of this paper (July 2002), we have used 100mm axial length for technology development and are completing infra-structure work that will make mirror segments with axial lengths of 200mm to 300mm possible.

## 2 Mirror Segments Requirements and Fabrication

Since the construction of the SXT assembly has two steps, the first being the fabrication of the mirror segments and the second being the integration and assembly of the segments, we have tentatively allocated an error budget for each of the two steps. One of important drivers behind the allocation of errors is to reduce the overall cost of constructing the SXT. In this section, we will briefly discuss these errors and the rationale behind their allocations.

### 2.1 Error Allocations

Each mirror segment is an aspherical surface: parabolic for the primary segments and hyperbolic for the secondary. Mathematically each surface can be described by a relation between its radius of curvature ( $r$ ) and axial distance ( $z$ ), as shown in Figure 2, where the  $z$ -axis coincides with the optical axis and its origin at the geometric center of the segment. The range of the segment in the optical axis direction is defined by  $-\frac{L}{2} \leq z \leq \frac{L}{2}$ , where  $L$  is the axial length/height of the segment which is 200mm in the current optical design. The primary and secondary segment can be described by

$$r_p = r_{p0} + \tan \alpha_p \cdot z + S_p \cdot \frac{2z^2}{L} + O\left(\frac{2z^3}{L}\right) \quad \text{and} \quad r_s = r_{s0} + \tan \alpha_s \cdot z + S_s \cdot \frac{2z^2}{L} + O\left(\frac{2z^3}{L}\right)$$

respectively, where the various parameters are self-explanatory. Strictly or mathematically, the corresponding parameters between the primary and secondary segments are all different. But in practice, only  $r_{p0}$  and  $r_{s0}$  are materially different and  $\alpha_s \approx 3\alpha_p$  and  $S_s \approx S_p$  and, in particular, the higher order terms can be neglected without any loss of angular resolution in the context of Constellation-X (Saha & Zhang, 2002, in preparation).

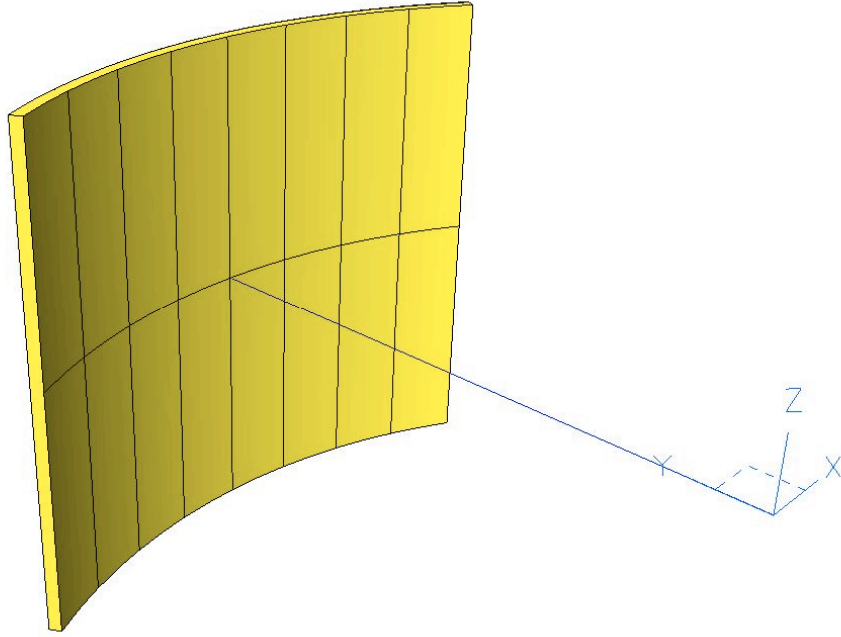


**Figure 2 Illustration of a mirror segment and its coordinate system used for its definition. The z-axis points up, y-axis through the center of the segment.**

### 2.1.1 Average Radius ( $r_{p0}$ or $r_{s0}$ ) Errors

Error in the average radius of a segment translates into a shift in image in the focal plane by the same amount. Given SXT's plate scale of 48.5  $\mu\text{m}$  per arc-second and the angular resolution requirement of 15" and taking into account that the alignment/assembly process can correct errors in average radii, we allocate  $\pm 100 \mu\text{m}$  to the average radius.

### 2.1.2 Average Slope (Cone Angles $\alpha_p$ and $\alpha_s$ ) Errors

The final image quality is very sensitive to these errors. Otherwise known as the  $\alpha\alpha\text{R}$  errors, they are correctable by the alignment/assembly process. As such we allocate  $\pm 30''$  to these errors. Two considerations have gone into this allocation. First, it is extremely expensive to make mirror segments with the cone angle error less than one arc-second that is required for the SXT (see discussion below on forming mandrel specifications). Second, the alignment/assembly procedure will change/disturb the intrinsic cone angle of the segment during the alignment process. The combination of these two facts dictate that the most cost-effective choice is to allow a large cone angle error for the segment which will then be corrected by the alignment/integration procedure.

### 2.1.3 Sag ( $S_p$ and $S_s$ ) Errors

These sags are responsible for the focusing power of the telescope. How they translate in terms of image quality depends on the statistical relationship between  $S_p$  and  $S_s$ . If they are statistically independent, the final image quality is relatively insensitive to their

errors, in which case we allocate  $\pm 0.3 \mu\text{m}$ . On the other hand, if they are correlated, i.e., they tend to err with the same sign, the final image quality is fairly sensitive to an error in them, in which case we allocate  $\pm 0.08 \mu\text{m}$ . The final resolution of this error allocation awaits the determination of the statistical properties of fabricated mirror segments.

#### 2.1.4 Axial Figure ( $\sigma_{\frac{2z}{L}}$ ) Errors

Also referred to as the residual figure errors, these are perhaps the most important errors. They measure the statistical distribution of mirror slope errors along the optical axis. The reflection process greatly amplifies this error. Each arc-second RMS error in axial slope error distribution translates into 3.9 arc-second half-power diameter in the final image quality. Therefore we require that the RMS slope error of the mirror segment must be less than  $2''$ .

#### 2.1.5 Microroughness Requirement

Microroughness of the mirror surface determines the X-ray scattering characteristics of the final image. It disproportionately affects the image quality at higher energies. Taking into account the final image requirement of 15 arc-second, we require a microroughness of less than 6 Angstroms measured in the band with spatial periods less than 0.3mm.

### 2.2 Technical Approach

Each mirror segment is fabricated using a two-step process: substrate formation and epoxy replication. We first slump a flat sheet of glass onto a convex forming mandrel to form a substrate. This substrate has a good large scale figure but has a lot of mid-frequency errors. Then we spray the substrate's inner surface with a layer of epoxy and mate it with a Au-coated precision replication mandrel. After the epoxy has been cured, the substrate plus the epoxy and the Au coating is separated from the replication mandrel. As such each segment derives its characteristics from two mandrels: a substrate forming mandrel and a replication mandrel. Table 2 lists the connections between the segment characteristics and the two mandrels.

**Table 2 Connections between the characteristics of the mirror segment and the mandrels.**

Segment Characteristics	Forming Mandrel	Replication Mandrel
Average Radius	X	
Average Slope (Cone Angle)	X	
Sag Precision	X	X
Axial Figure Precision		X
Microroughness		X

### 2.2.1 Substrate

The substrate is the part of the mirror segment that provides the necessary mechanical integrity. The most important properties it must possess are: (1) resilience and long term stability, (2) good large scale figure, and (3) meeting the mass requirement.

### 2.2.2 Material Selection

A variety of materials can potentially serve as the substrate material: metals (aluminum, titanium, nickel, etc.), composites, and glass. Each has its own distinctive advantages and disadvantages. We have selected glass for several reasons. First, glass is an ideal optical material with excellent stability. It is totally brittle and does not undergo plastic deformation. Therefore it can hold its figure well. Second, glass is light compared to metals. Third, glass is inexpensive and commercially available in the form we need. In particular, we have selected the D263 thin glass sheets manufactured by Schott. In composition, it is very similar to the regular Pyrex glass. It comes in large sheets, typically 430mm by 350mm, and in a large number of thicknesses: ranging from 30  $\mu$ m to 1,100  $\mu$ m. The mass requirement of the SXT mirror assembly dictates that, given the D263 density of 2.5 g/cm<sup>3</sup>, the glass thickness must not exceed 0.6mm. For technology development, we use 0.4mm thick D263 glass sheets. Similar materials have been used by other groups for making X-ray mirrors (Labov 1988 and Craig et al. 2000).

### 2.2.3 Forming Mandrels

To reduce cost, the forming mandrels are conical approximations of the underlying Wolter-I surfaces. Precision of the forming mandrel is relatively coarse compared to the typical optical mirrors, but it is substantially more stringent than machining technology can provide. Over the past two years, we have been working with Rodriguez Precision Optics, Inc., to fabricate forming mandrels out of commercial grade fused silica. Our experience so far has proven that (1) commercial fused silica is a satisfactory material for this purpose despite its porosity associated with many bubbles and (2) an axial straightness of peak to valley less than 2  $\mu$ m can be readily achieved.

### 2.2.4 Slumping

The slumping process takes a flat D263 glass sheet and molds it onto the conical surface of the forming mandrel. Several aspects are crucial for the success of slumping. First, the temperature ramping has to be sufficiently slow so that the forming mandrel is at thermal equilibrium at the temperature when D263 starts slumping under its own weight. Our experiments indicate that the temperature is about 540 degrees centigrade. Second, the slumping process has to take place in a relatively clean environment. Any dust particles trapped between the glass sheet and the forming mandrel surface will create dimples on the substrate. Third, the forming mandrel surface has to be properly treated to ensure that the substrate not stick to it. We have developed a proprietary procedure to treat a polished fused silica surface to prevent sticking.

In contrast to the conventional slumping *into* a concave mold (e.g., Craig et al. 2000), we have chosen to slump *onto* a convex mandrel. Slumping onto a convex mandrel has several advantages. First, it ensures that the inner surface of the substrate comes in

contact with the mandrel surface. Second, any thickness variations in the glass sheet do not translate into errors on the substrate surface of interest. Third, the slumping process from a flat sheet to a conical section is a very gradual one. As the temperature ramps up, the flat glass sheet just wraps gradually around the mandrel. There is no abrupt sagging that can cause “wrinkles” in the substrate.

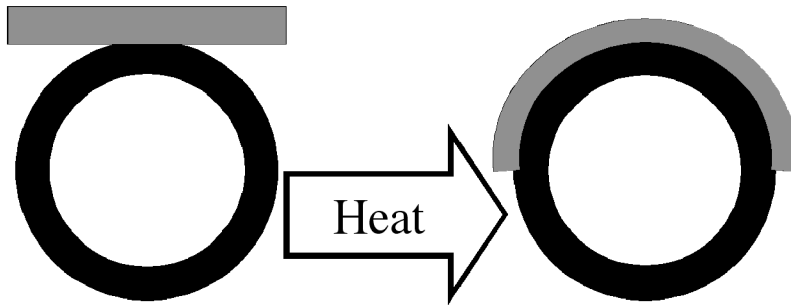


**Figure 3 Illustration of the glass slumping process. In contrast to the more conventional slumping into a mold, we have chosen to slump onto a convex mandrel because the inner surface of the substrate is of interest here.**

### **2.2.5 Precision Trimming**

After the glass sheet has slumped onto the forming mandrel surface and has cooled down to room temperature, we cut off all 4 edges of the substrate. This cutting-off of the edges as follows is necessary for two reasons. First, the edges are almost always inaccurately slumped compared to the inner parts of the glass because of gravity asymmetries. Second, the alignment and assembly process requires the edges of the mirror segment to be of sufficient quality. Last, but not least, we need to ensure the edges to be free of micro-fractures. We have developed a proprietary technique to perform this trimming operation while the substrate is still on the forming mandrel. We use the mandrel surface as the reference for performing the cutting. Figure 4 shows a precision cutting fixture that is being developed in collaboration with Swales Aerospace, Inc. It is based on a coordinate measuring machine. The glass-cutting tip is precisely aligned with the CMM measuring tip to ensure accuracy.



**Figure 4 A precision glass-cutting machine being developed in collaboration with Swales Aerospace, Inc. It is CMM-based and capable to cut curved as well as flat glass sheets.. Our proprietary scribing technique ensures the edges are free of micro-fractures.**

As a quality check, each substrate is measured with an interferometer or a laser scanner at 5 azimuthal positions which approximately correspond to  $5^\circ$ ,  $18^\circ$ ,  $31^\circ$ ,  $44^\circ$ , and  $55^\circ$  for a  $60^\circ$  segment. Figure 5 shows the axial figure measurements of a typical substrate. There are two characteristics worth noting. First, the mid-frequency ripples are on the order of  $0.2\mu\text{m}$  as indicated by the number under the RMS column. Most likely these ripples result from the “buckling” of the glass surface as part of the slumping. Second, overall the axial measurements indicate that the substrate is very straight in the optical axis direction. The second order curvature is very small indeed as indicated by the numbers under the Sag column. Figure 6 shows the distribution of many sags measured from many different substrates. They follow a normal distribution centered on the sag of the mandrel with a standard deviation of  $0.37\mu\text{m}$ .

Figure 5 and Figure 6 show our glass slumping capability as of July 2002. These substrates have not yet been replicated. In the next sections, we report on our replication technique and the quality of replicas from work done several months ago.

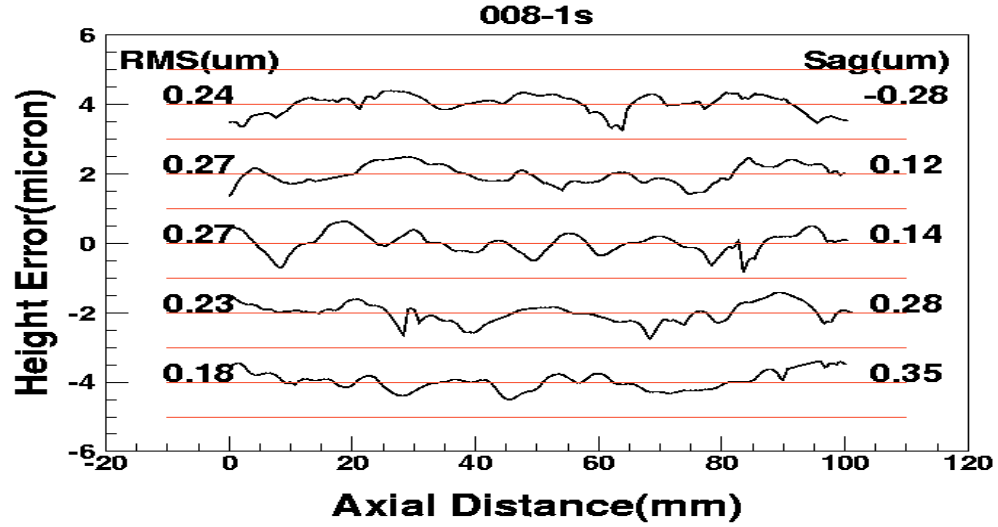


Figure 5 Five axial figure measurements of a typical substrate. Each measurement is fit to the function  $P_0 + A \cdot P_1 + B \cdot P_2$ , where  $P_0$ ,  $P_1$ , and  $P_2$  are Legendre polynomials of 0th, 1st, and 2nd order. The number under the Sag column is the coefficient of the 2nd order polynomial. The number under the RMS column is computed after the removal the polynomial fit. They characterize the residual figure errors, or waviness of the substrate.

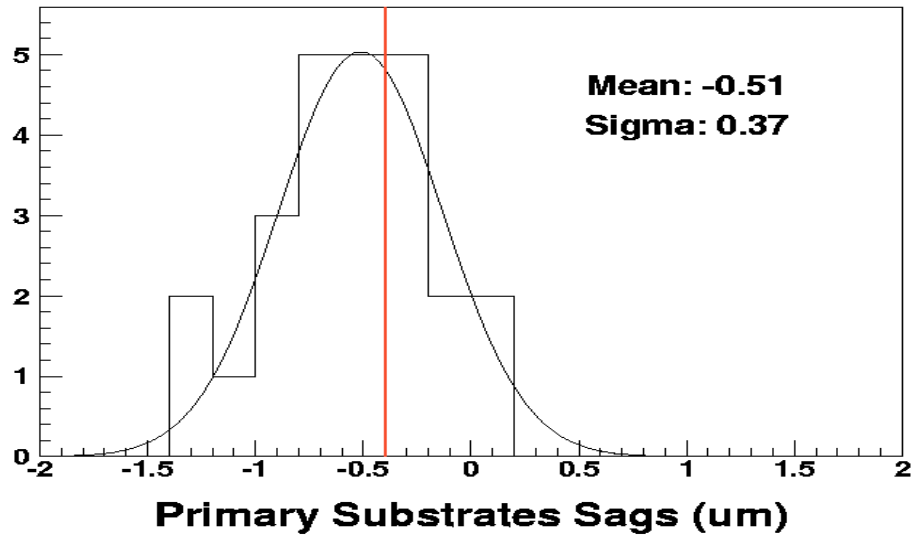


Figure 6 Distribution of substrate sags (defined as the coefficient of the fit to the 2<sup>nd</sup> order Legendre polynomial) in comparison with that of the forming mandrel. The vertical line at -0.4 is the sag of the forming mandrel.

## **2.3 Replication**

The substrates formed in the slumping process described in the last section have errors that need to be corrected by an epoxy replication procedure. First, their mid-frequency ripples need to be smoothed out. Second, their sags are distributed around that of the forming mandrel that is not accurate enough. The replication process smoothes out the ripples and imparts the correct sag to the segment.

The replication is a three-step process. First, a thin layer of epoxy is sprayed on the inner surface of the substrate. Second, the substrate is brought into contact with a Au-coated replication mandrel in a vacuum chamber. Third, moderate heat is applied to the mated substrate and replication mandrel to cure the epoxy. After the epoxy is cured, the mirror segment is peeled off from the replication mandrel. The essentials of this process have been developed and matured for fabricating Astro-E mirrors (Chan, Soong, & Serlemitsos 2002).

### **2.3.1 Replication Mandrels**

The mirror segment derives its sag, residual or mid-frequency figure error, and microroughness from the replication mandrel. As such the replication mandrel must at least meet, and better yet, exceed the requirements imposed on the mirror segment. In addition, the replication mandrel must also meet other physical and chemical requirements that would make possible separation of the segment and fabrication of many segments off the same mandrel. Our experience indicates that replication mandrels made of glass (BK7, Pyrex, etc) or glass ceramics (Zerodur etc.) are much preferred to those fabricated out of metals, e.g. Ni. At issue is the adhesion between the X-ray reflecting material, e.g., Au, and the mandrel material. High adhesion makes it difficult, or even impossible, to separate the mirror segment from the mandrel. When separation is possible, high adhesion results in unacceptable microroughness and distortion of the final separated mirror segment. Our experience indicates that the distortion introduced during the separation can take hours to days to dissipate. It is not clear whether the distortion completely disappears. High adhesion also leads to the degradation of the mandrel microroughness. For an electroless nickel surface, epoxy replication with Au as the release layer can degrade the mandrel microroughness by a factor of 2 in as few as half a dozen replications. On the other hand, glass mandrels do not appear to degrade at all. Our experience with the fabrication of Astro-E mirrors indicates that glass mandrels can sustain hundreds of replications without any sign of degradation.

For technology development in the next few years, we will use both Ni and Zerodur mandrels fabricated by Zeiss. Currently the Constellation-X project has available two Ni mandrels which have a diameter of 0.5m and focal length of 8.4m. Zerodur is the preferred material for its well-understood optical and mechanical and thermal properties. A vast amount of knowledge and experience has been accumulated over the past three decades in grinding, figuring, and polishing Zerodur.

### 2.3.2 Application of Epoxy

The epoxy layer serves two purposes. First, it fills the gap between the substrate and the replication mandrel. Second, it serves as a bonding agent to attach the X-ray reflecting layer (e.g. Au) to the substrate. This layer has to be thick enough to smooth out the mid-frequency ripples of the substrate *and* to bridge the difference between the nominally conic surface of the substrate and the precisely curved replication mandrel. On the other hand, the epoxy layer introduces a bi-layer effect. Its thickness should be minimized to reduce the temperature sensitivity of the final mirror segment. In addition, the epoxy curing process builds up internal stress which can distort the segment figure. Given the quality of the substrate as described above, it takes no more than a couple of microns of epoxy to smooth out the mid-frequency ripples. The largest sagittal depth of the SXT mirror segments is about 3 microns for the 200-mm axial length. To form this 3-micron curvature, at least 10-micron epoxy is needed. Currently we baseline our process with a 10-micron epoxy thickness with an intention to reduce it further if possible.

The application of the epoxy is accomplished by spraying. In order to be sprayable, the epoxy is mixed and diluted with toluene. Figure 7 shows an automated spray system.

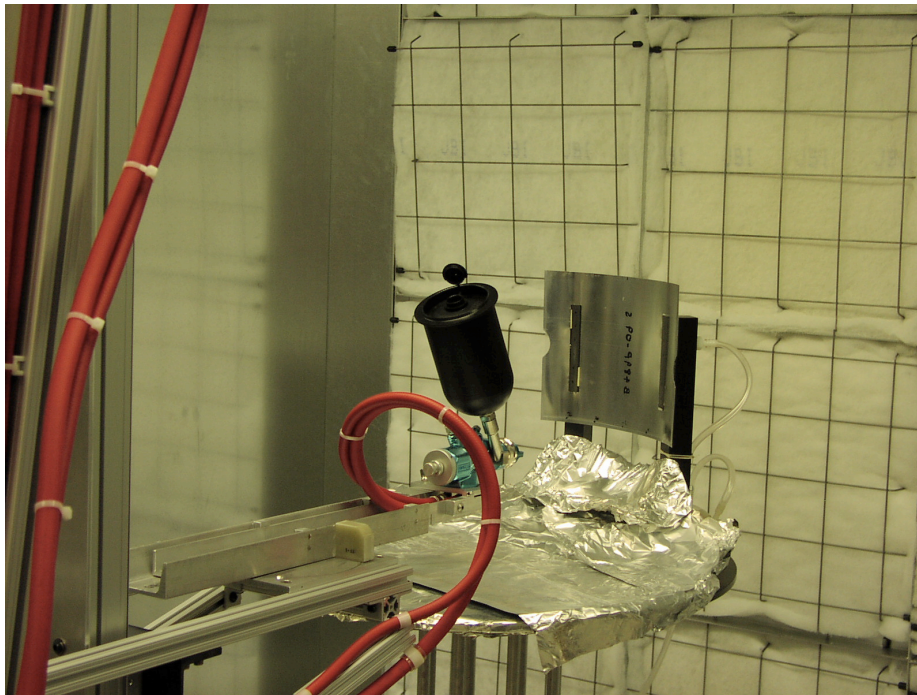


**Figure 7 A robotically controlled epoxy spray system. The system is engineered to achieve a very thin, uniform, and consistent epoxy layer on the substrate which is shown on the right.**

### 2.3.3 Mating and Separation of Substrate and Mandrel

The epoxy-coated substrate and the Au-coated replication mandrel are brought together in a vacuum chamber. This mating in vacuum is necessary for two reasons: (1) to

eliminate air pockets in the epoxy layer, and (2) to facilitate the flow of epoxy from one area to another. Figure 8 shows the replication chamber. In this particular design, the replication mandrel actually serves as part of the vacuum chamber.

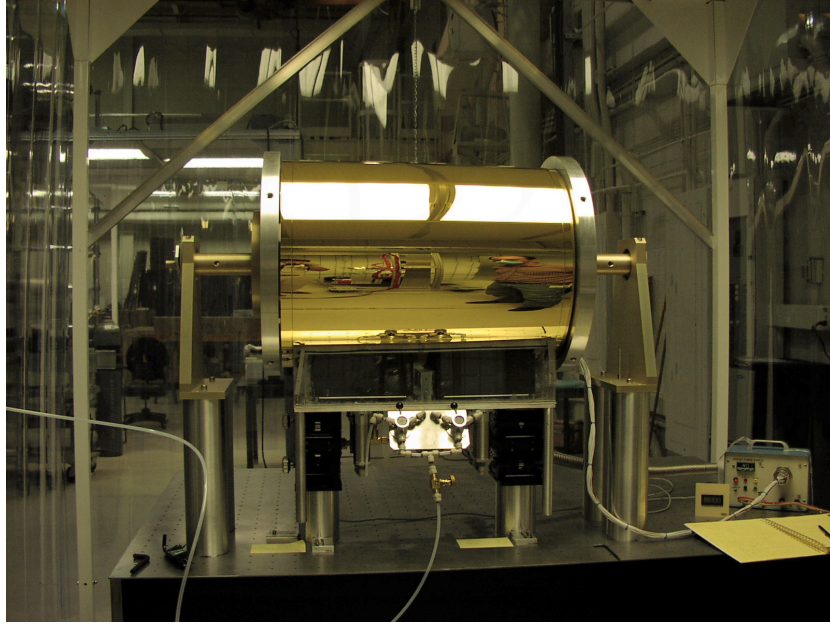


**Figure 8** This picture shows that the substrate and the replication mandrel have been brought together. The lower part is the vacuum chamber. In this setup, the replication mandrel serves as part of the vacuum chamber.



**Figure 9** After the epoxy has cured, separating the replica from the replication mandrel is straightforward by pulling from a corner.

### 2.3.4 Fidelity of the Replication Process

The fidelity of the replication process is characterized by three quantities: (1) the mirror segment's surface microroughness, (2) the mirror segment's residual axial figure error, and (3) the mirror segment's sag error.

In general we have found that microroughness is nearly perfectly replicated from the replication mandrel within one Angstrom of RMS. Our experience also indicates that pure electroless Ni surface is not amenable to replication.

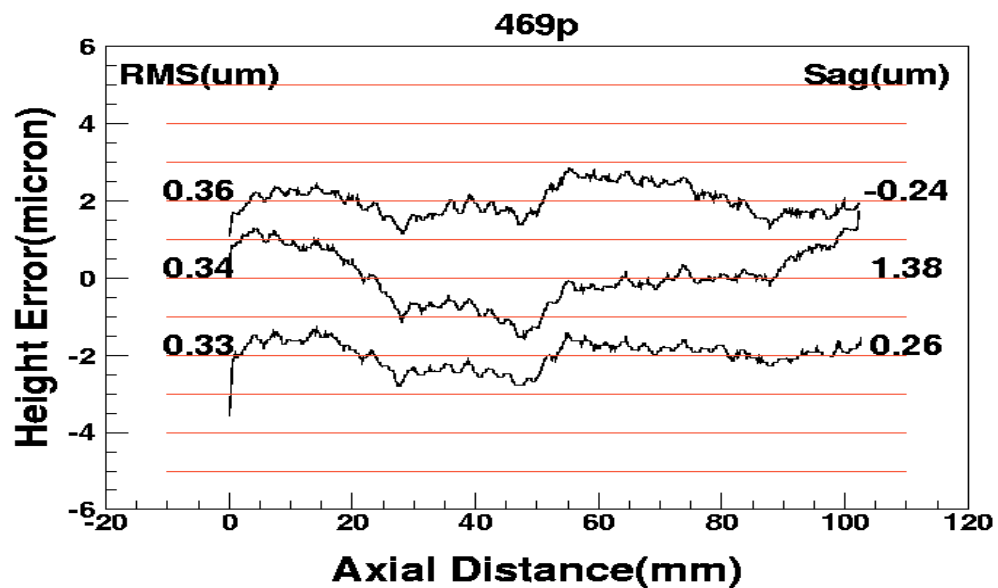


**Figure 10 Three axial scans of a formed substrate before replication. The high frequency jaggedness is due to the laser scanner used for these measurements.**

Figures 10 and 11 show, respectively, axial scans of a mirror segment in substrate form and in replicated form. It can be seen that the replication process changed both the sags and eliminated the residual figure errors. Figure 12 shows the distribution of the residual figure, or slope, errors. The nearly equal RMS values between the replica and the mandrel mean attest to the fidelity of the replication process.

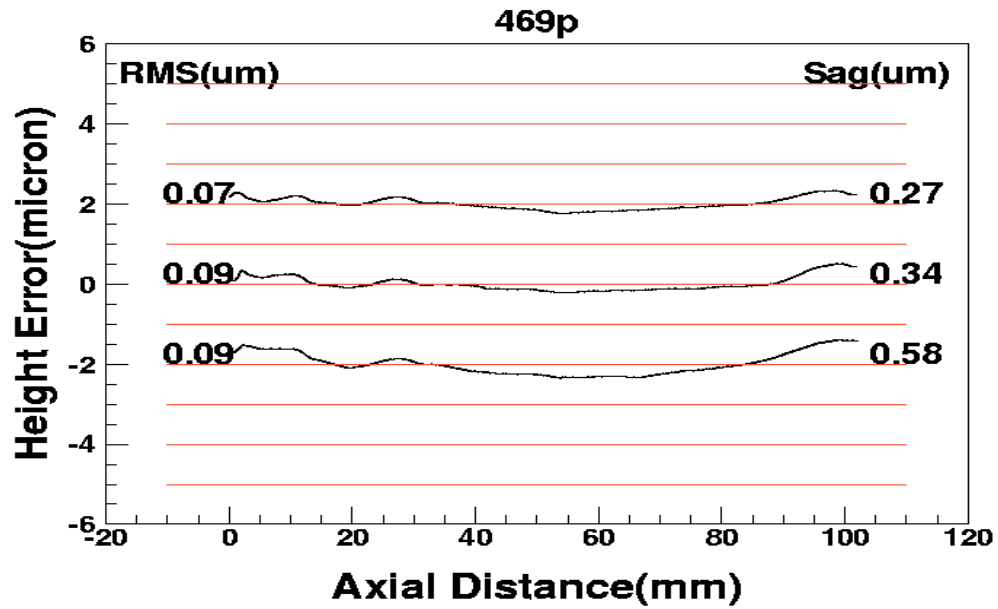
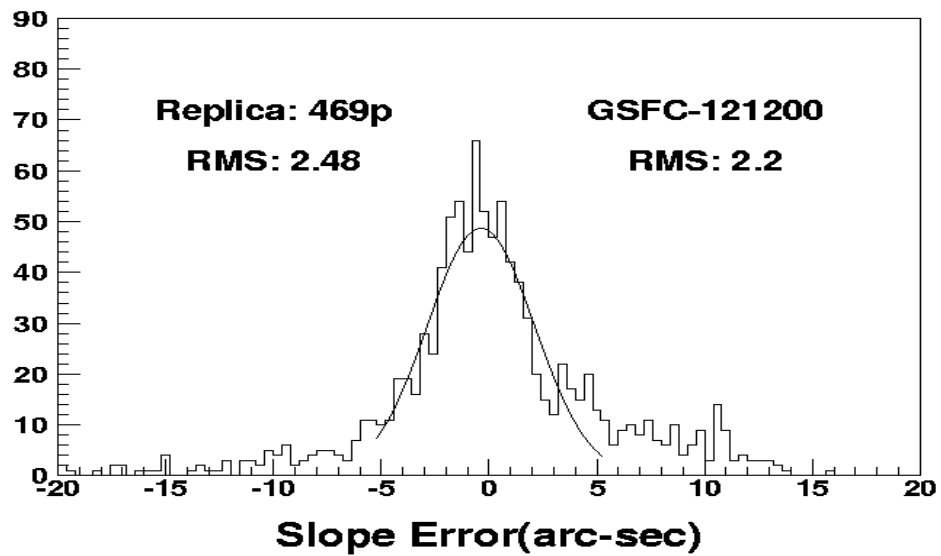


Figure 11 The substrate shown in Figure 10 after replication. The small ripples here are due to the replication mandrel itself.



### 3 Development Status

This paper is a snapshot of a rapidly evolving development process. Things change from week to week. As of the writing of this paper (July 2002), we are on the verge of demonstrating conclusively that the process outlined in this paper can meet, and likely

exceed, the requirements of SXT, at least with mirror segments of axial length about 100mm. The obstacles are mainly logistical. In this section, we list factors as we see at the present time that are important and that we will address in the immediate future.

### ***3.1 Process Development***

Process development in the next couple of years has two important aspects: (1) to demonstrate conclusively the meeting of the requirements with mirror segments of larger sizes and (2) to improve efficiency and achieve the highest cost-effectiveness possible. On the first aspect, we will take delivery in the next few months both forming and replication mandrels for the largest possible SXT shells. It is generally accepted that once we demonstrate that we can make the largest mirror segments, then we can make all mirror segments. On the second aspect, we will critically examine each step of the process to identify ways to achieve efficiency and reliability. Fabricating more than 15,000 precision mirror segments no doubt will be a challenge. Every step of the process will need to be optimized for efficiency and reliability.

### ***3.2 Prototype Mirror Segments***

As part of the demonstration for technology readiness for a flight program, we have on order three segmented replication mandrels that have nominal diameters of 1.6m, 1.2m, and 1.0m. We will use these mandrels to fabricate mirror segments that will populate two outer modules. They will be used for test and verification of the alignment/integration procedures.

### ***3.3 Important Issues***

Constellation-X will probably be the first mission to fly very thin glass mirrors in space. There are a number of important issues that need to be addressed. Here we discuss two most important ones: glass strength and outgassing.

#### ***3.3.1 Glass Strength***

Small defects and fractures in glass sheets can propagate and cause catastrophic breakage of a whole sheet. Our preliminary experiments have shown that the slumping process appears to weaken the glass sheets by as much as a factor of two. We are investigating the mechanism of this weakening and experimenting ways of increasing the strength of the slumped pieces. We are investigating an acid etching process to remove all fractures and defects after slumping.

#### ***3.3.2 Epoxy Outgassing***

Epoxy is a volatile substance and can cause contamination problems in a space flight environment. There are at least two ways in which the epoxy in the mirror segments can cause potential problems: (1) condensation on the X-ray reflecting surface that reduces/diminishes its X-ray reflectivity and (2) condensation on cryogenic detectors and their blocking filters that reduces X-ray detection quantum efficiency and transmission. Our experience and tests in the past several years have indicated that the effect on reducing X-ray reflectivity is not a problem at all. The condensation on detector filters and similar cryogenic surfaces needs to be investigated.

## 4 Future Considerations

Constellation-X requires an angular resolution of 15" (HPD). Its goal is actually to reach 5" (HPD) to enhance its scientific return. It is not clear at the present what is the practical fundamental limit on angular resolution we can achieve with the technique described here. We will continue to refine each step of the process with an aim to improve and understand any obstacles to better angular resolution. The crucial factors here are: (1) substrate quality which is directly coupled with the forming mandrel quality, (2) epoxy application technique in reducing thickness and improving uniformity, (3) precision in mating substrate and replication mandrel.

## 5 Acknowledgements

Many people at different institutions have contributed to the work reported in this paper. It is not possible to list them all. In particular we want to express our thanks to Steve O'Dell, Bill Jones, and Dwight Goodman of the Marshall Space Flight Center, Bill Podgorski and Bill Davis of SAO, and Diep Nguyen, Curtis Odell, Jim Mazarella and Dave Colella of the Goddard Space Flight Center. We thank Chuck Katz for presentation and editorial suggestions.

## 6 References

Chan K., Soong Y., and Serlemitsos P.J., paper 4851-52, in these proceedings

Craig W.W, et al. 2000, Opt Express 7 (4): 178-185

Hair, J., et al. 2002, paper 4851-76, in these proceedings

Labov S.E., 1988, Appl Optics 27 (8): 1465-1469

Podgorski, W., 2002, paper 4851-57, in these proceedings

Serlemitsos P. J., and Soong Y., 1996, Astrophysics and Space Science, Vol. 239, p. 177